Pin-wise Reactor Analysis Based on the Generalized Equivalence Theory

Hwanyeal Yu, Woong Heo, and Yonghee Kim[a*]
[a] *Department of Nuclear & Quantum Engineering, KAIST, Daejeon, Republic of Korea*
[*] *Corresponding author: yongheekim@kaist.ac.kr*

1. Introduction

Recently, high-fidelity multi-dimensional analysis tools are gaining more attention because of their accurate prediction of local parameters for core design and safety assessment. In terms of accuracy, direct whole-core transport is quite promising. However, it is clear that it is still very costly in terms of the computing time and memory requirements. Another possible solution is the pin-by-pin core analysis in which only small fuel pins are homogenized and the 3-D core analysis is still performed using a low-order operator such as the diffusion theory.

In this paper, a pin-by-pin core analysis is performed using the hybrid CMFD (HCMFD) method [1]. Hybrid CMFD is a new global-local iteration method that has been developed for efficient parallel calculation of pin-by-pin heterogeneous core analysis. For the HCMFD method, the one-node CMFD [2] scheme is combined with a local two-node CMFD method in a non-linear way.

In pin-by-pin core analysis, the multi-group constants can be produced by using the well-developed the generalized equivalence theory (GET) [3,4,5] or the group cross sections can be corrected by the super-homogenization method (SPH) [6,7]. Regarding application of the GET theory to the pin-by-pin core analysis, K.W Park, et al [8] did a feasibility study using the finite difference method (FDM), which requires a very small mesh size for accuracy. Meanwhile, Yamamoto et al. showed that error of the whole core pin-wise calculation can be noticeably reduced by using the SPH method. Since the SPH method is iterative and SPH factors are not direction dependent, it is clear that SPH method takes more computing cost and cannot take into account the different heterogeneity and transport effects at each pin interface. Unlike the SPH method, the GET is non-iterative, discontinuity factors can be determined in a single step, if the reference solution is given. And the GET provides four different discontinuity factors that contain information about the orientation and position of the pin in its neighborhood.

In this research, the pin-wise discontinuity factors are determined using the NEM (Nodal Expansion Method) method to improve the accuracy and reduce the computing time of the pin-by-pin core analysis.

2. Fuel Assembly Analysis for Pin Homogenization

In order to get 2-group homogenized pin-wise cross-sections and the associated discontinuity factors of each pin, two types of 17x17 Westinghouse type fuel assembly calculations (4.9% and 3.0% enrichment) are performed using the Monte Carlo Serpent2 code with the ENDF/V-VII.0 data library. Figure 1 shows the 17x17 fuel assembly layout and corresponding boundary conditions.

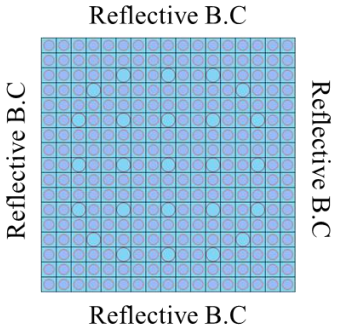

Fig. 1. Fuel assembly for pin-wise homogenization

In this study, the pin-wise discontinuity factors (PDF) are calculated on each side of every pin by using the well-known definition:

$$\mathrm{PDF} = \frac{\Phi_s^{het}}{\Phi_s^{\mathrm{hom}}} \cdot \tag{1}$$

Since the heterogeneous surface fluxes are determined using a high-order transport method, the PDFs in Eq. (1) depend on the method to determine the homogenous surface flux. For efficient pin-wise diffusion calculations, the homogeneous surface fluxes of each pin are calculated using a pin-level NEM nodal method.

The homogenized pin-wise cross-sections and pin discontinuity factors are tested on two types of fuel assemblies. FA-1 is loaded with 4.9% enriched UO_2 fuel and FA-2 is loaded with 3.0% enriched UO_2 fuel. Figure 2 shows calculated two-group pin-wise discontinuity factors of 1/8 fuel assembly FA-2. It is worthwhile to note that PDFs noticeably deviate from 1.0 and the actual discontinuity (ratio of two PDFs) is quite close to 1.0 on most of the surfaces except for the guide thimbles.

Table I shows that the two-group diffusion HCMFD calculation with pin discontinuity factors almost reproduces the reference solution, while the analysis without any PDFs results in a noticeable discrepancy in the eigenvalue. It should be noted that the HCMFD results include small stochastic uncertainty of the

reference solution since the reference calculations are calculated using the Monte Carlo method.

g=1 g=2	Left boundary 3.0%, Unrodded						
							0.995 1.051
						0.995 1.051	0.995 1.051
					0.993 1.053	0.995 1.051	0.995 1.051
				1.006 0.990	0.990 1.067	0.994 1.053	0.995 1.051
			0.993 1.052	0.994 1.045	0.993 1.048	0.994 1.054	0.995 1.052
		1.006 0.989	0.990 1.067	0.995 1.047	1.006 0.990	0.990 1.068	0.994 1.053
	0.994 1.050	0.994 1.043	0.993 1.053	0.994 1.049	0.994 1.044	0.993 1.053	0.994 1.052
0.993 1.053	0.994 1.050	0.993 1.044	0.993 1.053	0.994 1.049	0.994 1.044	0.993 1.053	0.994 1.052
1.005 0.989	0.990 1.067	0.995 1.048	1.005 0.989	0.990 1.067	0.995 1.048	1.006 0.989	0.990 1.068	0.994 1.053

g=1 g=2	Right boundary 3.0%, Unrodded						
							0.995 1.051
						0.995 1.051	0.995 1.051
					0.994 1.049	0.995 1.051	0.995 1.051
				1.006 0.990	0.995 1.044	0.994 1.050	0.995 1.051
			0.993 1.053	0.993 1.047	0.994 1.044	0.995 1.050	0.994 1.051
		1.006 0.989	0.995 1.048	0.989 1.066	1.006 0.989	0.996 1.046	0.995 1.051
	0.993 1.052	0.994 1.044	0.994 1.050	0.993 1.052	0.994 1.043	0.995 1.050	0.995 1.051
0.994 1.050	0.993 1.053	0.994 1.044	0.994 1.050	0.993 1.052	0.994 1.044	0.995 1.050	0.994 1.051
1.005 0.989	0.995 1.048	0.990 1.067	1.005 0.989	0.995 1.048	0.990 1.066	1.005 0.989	0.996 1.046	0.995 1.051

g=1 g=2	Top boundary 3.0%, Unrodded						
							0.995 1.051
						0.995 1.051	0.995 1.050
					0.993 1.053	0.994 1.050	0.995 1.050
				1.006 0.990	0.994 1.047	0.994 1.049	0.994 1.050
			0.993 1.052	0.994 1.048	0.990 1.066	0.994 1.053	0.994 1.050
		1.006 1.989	0.994 1.044	0.994 1.043	1.006 0.989	0.994 1.045	0.994 1.048
	0.994 1.050	0.995 1.048	0.994 1.050	0.994 1.050	0.995 1.048	0.995 1.050	0.995 1.050
0.993 1.053	0.993 1.053	0.990 1.067	0.993 1.053	0.993 1.053	0.990 1.067	0.993 1.053	0.994 1.050
1.005 0.989	0.994 1.044	0.994 1.044	1.006 0.990	0.994 1.044	0.994 1.044	1.006 0.989	0.994 1.045	0.994 1.048

g=1 g=2	Down boundary 3.0%, Unrodded						
							0.995 1.051
						0.995 1.051	0.995 1.051
					0.994 1.049	0.994 1.051	0.994 1.051
				1.006 0.990	0.994 1.045	0.994 1.049	0.994 1.050
			0.993 1.053	0.990 1.066	0.995 1.049	0.994 1.049	0.994 1.050
		1.006 0.989	0.993 1.045	0.993 1.046	1.005 0.990	0.994 1.045	0.994 1.048
	0.993 1.052	0.990 1.067	0.993 1.053	0.993 1.053	0.990 1.067	0.993 1.053	0.994 1.050
0.994 1.050	0.994 1.050	0.995 1.048	0.995 1.050	0.994 1.050	0.995 1.048	0.995 1.050	0.995 1.050
1.005 0.989	0.994 1.044	0.994 1.044	1.006 0.990	0.994 1.044	0.994 1.044	1.006 0.989	0.994 1.045	0.994 1.048

Fig. 2. Pin-wise two-group PDFs in 1/8 FA-2 fuel assembly

Table I: Summary of single assembly calculation.

FA type & method		k-inf	Error in k-inf, pcm
FA-1 (Ref. Serpent2)		1.413992 ± 0.000005	Ref.
HCMFD	without DF	1.415192	59.96
	with all DF	1.413988	-0.21
FA-2 (Ref. Serpent2)		1.325470 ± 0.000006	Ref.
HCMFD	without DF	1.326698	69.79
	with all DF	1.325459	-0.66

3. Application to a Small PWR Core Benchmark

3.1 Benchmark problem

To test the feasibility of the GET-based pin-by-pin core analysis with pin-wise homogenized parameters and PDFs, a small two-dimensional PWR quarter core benchmark, which is similar to the EPRI-9 problem [9] is considered. The fuel assemblies of the EPRI-9 problem are replaced with the two 17x17 fuel assemblies described in Table I. Figure 3 shows the layout of the modified EPRI-9 benchmark problem. Figure 3 includes different five sets of baffle and reflector regions (B1~B5 and W1~W5) which will be used in the sensitivity study in Section 3.2.

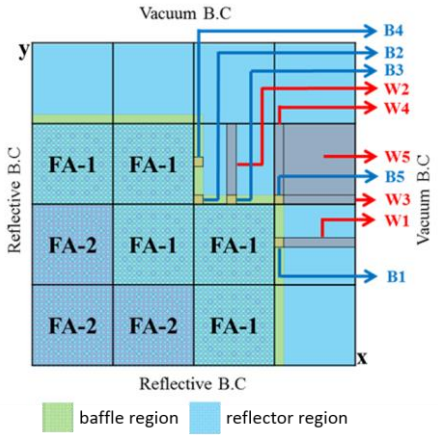

Fig. 3. Quarter core layout of the modified EPRI-9 benchmark

Since this modified EPRI-9 benchmark contains the baffle and water reflector, the 2-group cross-sections and discontinuity factors of the baffle and reflector regions are also calculated with the conventional approach. Figure 4 shows the spectral geometry used for calculating the 2-group parameters of the baffle and reflector regions. It should be noted that energy condensation is only done for in the baffle and reflector regions without any homogenization. For determination of the discontinuity factors of the baffle and reflector regions, the 2-group homogeneous surface fluxes are also calculated using the standard 1-D NEM kernel considering the node balance, first and second moment node balance and two-side boundary conditions from

two sides.

It should be noted that there is an L-shaped baffle-water reflector in the modified EPRI-9 benchmark problem. However, the same 2-group parameters from the simple spectral geometry are simply applied to the L-shaped baffle-water reflector regions as in the conventional 2-step reactor core analysis in this work.

Table II tabulates the two-group discontinuity factors of the baffle and reflector regions. It is clear that discontinuity factors of the baffle and reflector are quite different from the unity unlike the discontinuity factors of fuel pins. This means that the role of discontinuity factors of the baffle-reflector regions is important in the pin-wise core calculations.

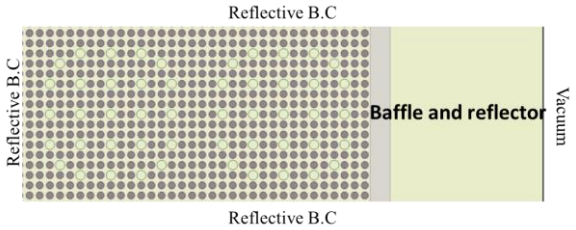

Fig. 4. Spectral geometry for baffle and reflector analysis

Table II: Discontinuity factors of baffle and reflector region

	Baffle DF		Reflector DF
Energy group	Reflector side	Fuel side	Baffle side
1st group	0.981	1.023	1.121
2nd group	1.022	1.051	1.036

3.2 Results of the 2-D core analysis

Based on the 2-group cross-sections and associated discontinuity factors on each surface from the fuel assembly and simple baffle-reflector model analyses, the small PWR core was analyzed with the HCMFD algorithm and the numerical results are summarized in Table III. In Table III, several sets of the HCMFD solutions are given, which are different in using the DF information: without any DF, with DF only applied on the fuel assembly regions, with DF only applied on the baffle-reflector regions, and finally with all PDFs applied on both fuel and baffle-reflector regions.

It is noted in Table III that the k-eff error is relatively small even with no DF applications and it becomes even bigger when PDFs are only applied to the fuel regions, while DFs for the baffle-reflector regions improves the k-eff prediction. The DF-dependency of the solution can be understandable by recalling that PDF for the fuel pins are obtained from the infinite fuel assembly analysis and the baffle-reflector DFs were determined in a relatively more realistic model. Nevertheless, Table III also clearly indicates that DFs should be used in both fuel and non-fuel regions for a higher accuracy.

Figures 5 and 6 show the pin power error distribution in the modified EPRI-9 benchmark without and with pin discontinuity factors. Figure 7 shows the fuel assembly power error and maximum pin power errors in each fuel assembly as well as the normalized assembly power profile of the core. From Figs. 5, 6, and 7, one can note that the pin-wise discontinuity factors clearly reduce the maximum errors in the pin power at the edge of the core, from about 5% to ~3%. This means that the baffle reflector discontinuity factors and 2-group parameters are working correctly for the pins directly adjacent to the baffle-reflector region. The correcting effect of these baffle reflector 2-group parameters is limited, however, only to the peripheral pins as there is a significant error in the calculated pin-power in the inner pins of the peripheral assemblies. One can note that as the power in the pins neighboring the baffle-reflector region is increased, the power in the inner pins of the peripheral fuel assemblies also increases, which in turn increases their calculated error.

The opposite effect is seen in the inner fuel assemblies. Since the 2-group constants are generated from single fuel assembly calculation, they cannot correctly reflect the neighborhood effects. As expected, it is found that the maximum pin power error occurs at the corner of fuel assemblies where two different fuel assemblies are in contact. Of note is the increased error in the center most fuel assembly with the implementation of the discontinuity factors. This is because with the increase in peripheral assembly power, the relative power of the inner assemblies should decrease. This in turn increases the difference from the reference solution and therefore error in calculated pin-power.

Table III: Result of modified EPRI-9 problem

method		k-eff	Error in k-eff, pcm
Ref. Serpent2		1.273951 ± 0.000005	Ref.
HCMFD	without DF	1.272188	-108.8
	with FA DF only	1.270841	-192.1
	with baffle-reflector DF only	1.274069	50.4
	with all DF	1.273408	-33.5

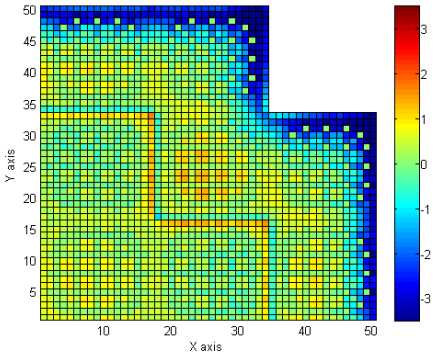

Fig. 5. Distribution of pin power error (%) in fuel region of modified EPRI-9 benchmark without pin discontinuity factors

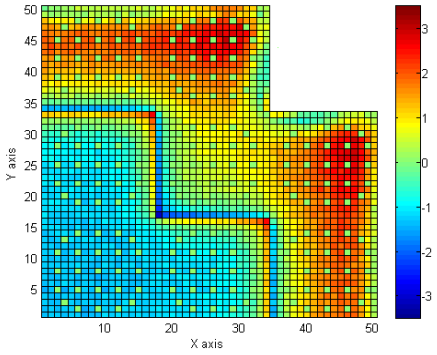

Fig. 6. Distribution of pin power errors (%) in fuel region of modified EPRI-9 benchmark with pin discontinuity factors

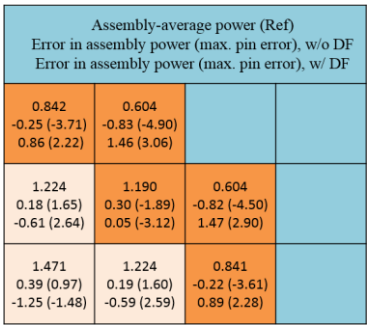

Fig. 7. Fuel assembly power error and maximum pin power error (%) in each fuel assembly

3.3 Impacts of baffle and reflector cross sections

In the above analysis of the modified EPRI-9 benchmark, a single set of baffle and reflector cross sections and DFs is used for both the flat and L-shape baffle-reflector regions. However, it is clear that the homogenized cross-sections of the baffle-reflector are space-dependent. To evaluate the impacts of the space-dependent cross-sections of the baffle and reflector on the core analysis, five sets of different baffle-reflector cross-sections are determined from the reference Serpent calculation, as shown in Fig. 3. Five different cross-section sets are applied to the corresponding locations. Table IV shows the results of the sensitivity analyses on the baffle-reflector cross sections. It is noted that the impact of space-dependent cross-sections on the k-eff value is quite small, which is only around 2 pcm in terms of the reactivity difference.

Table IV: Impacts of space-dependent baffle and reflector cross-sections

method		k-eff	Error in k-eff, pcm
Ref. Serpent2		1.273951 ± 0.000005	Ref.
HCMFD	without DF	1.272163	-110.3
	with FA DF only	1.270817	-193.6
	with baffle-reflector DF only	1.274747	49.0
	with all DF	1.273387	-34.8

3. Conclusions

In this paper, a pin-wise reactor analysis is performed based on the generalized equivalence theory. From the conventional fuel assembly lattice calculations, pin-wise 2-group cross sections and pin DFs are generated. Based on the numerical results on a small PWR benchmark, it is observed that the pin-wise core analysis provide quite accurate prediction on the effective multiplication factor and the peak pin power error is bounded by about 3% in peripheral fuel assemblies facing the baffle-reflector. Also, it was found that relatively large pin power errors occur along the interface between clearly different fuel assemblies. It is expected that the GET-based pin-by-pin core calculation can be further developed as an advanced method for reactor analysis via improving the group constants and discontinuity factors.

REFERENCES

[1] S.H. Song, "Pin-by-Pin Core Calculation with NEM-Based Two-Level CMFD Algorithm", MS Thesis, KAIST (2016)
[2] H.C. Shin and Y. Kim, "A Nonlinear Combination of CMFD (Coarse-Mesh Finite Difference) and FMFD (Fine-Mesh Finite Difference) Methods", *Proceeding of Korean Nuclear Society*, Spring Meeting, Pohang, Korea, May, 1999
[3] K. Koebke, "A New Approach to Homogenization and Group Condensation", IAEA-TECDOC-231, IAEA Technical Committee Meeting on Homogenization Methods in Reactor Physics, Lugano, Italy, November 13-15, 1978
[4] K. S. Smith, "Assembly Homogenization Techniques for Light Water Reactor Analysis," *Progress in Nuclear Energy*, 17, 303, 1986
[5] K.S Smith, "Spatial Homogenization Methods for Light Water Reactor Analysis", PhD Thesis, Massachusetts Institute of Technology (1980)
[6] A. Hebert, "A Consistent Technique for the Pin-by-Pin Homogenization of a Pressurized Water Reactor Assembly", *Nucl. Sci. Eng.*, 113, 227, 1993
[7] Akio, Yamamoto, et al, "Improvement of the SPH Method for Pin-by-Pin Core Calculation", Journal of Nuclear Science and Technology, Vol. 41, No. 12, p.1155, Dec, 2004
[8] K.W. Park, C.J. Park, K.T. Lee and N.Z. Cho, and Y. Kim, "Pin-cell Homogenization via Generalized Equivalence Theory and Embedding Assembly Calculation". Trans. Am. Nucl. Soc., Vol86, p.417, 2002
[9] H.S. Khalil, "The Application of Nodal Methods to PWR Analysis", PhD. Thesis, Department of Nuclear Engineering, Massachusetts Institute of Technology, Cambridge, MA (1983).